Invited article for Science

LBL-2283
Preprint c.2

JOSEPHSON JUNCTION DETECTORS

John Clarke

RECEIVED
LAWRENCE
RADIATION LABORATORY

JAN 29 1974

LIBRARY AND
DOCUMENTS SECTION

October 1973

Prepared for the U. S. Atomic Energy Commission
under Contract W-7405-ENG-48

TWO-WEEK LOAN COPY

This is a Library Circulating Copy which may be borrowed for two weeks. For a personal retention copy, call Tech. Info. Division, Ext. 5545

LAWRENCE BERKELEY LABORATORY
UNIVERSITY OF CALIFORNIA
BERKELEY

LBL-2283
c.2

DISCLAIMER

This document was prepared as an account of work sponsored by the United States Government. While this document is believed to contain correct information, neither the United States Government nor any agency thereof, nor the Regents of the University of California, nor any of their employees, makes any warranty, express or implied, or assumes any legal responsibility for the accuracy, completeness, or usefulness of any information, apparatus, product, or process disclosed, or represents that its use would not infringe privately owned rights. Reference herein to any specific commercial product, process, or service by its trade name, trademark, manufacturer, or otherwise, does not necessarily constitute or imply its endorsement, recommendation, or favoring by the United States Government or any agency thereof, or the Regents of the University of California. The views and opinions of authors expressed herein do not necessarily state or reflect those of the United States Government or any agency thereof or the Regents of the University of California.

Invited article for Science Magazine

LBL-2283
Preprint

UNIVERSITY OF CALIFORNIA

Lawrence Berkeley Laboratory
Berkeley, California

AEC Contract No. W-7405-eng-48

JOSEPHSON JUNCTION DETECTORS

John Clarke

October 1973

JOSEPHSON JUNCTION DETECTORS

Josephson devices are sensitive detectors of magnetic fields, voltages, and far infrared radiation

John Clarke

The author is professor of physics at the University of California, Berkeley, California 94720, and principal investigator at the Inorganic Materials Research Division of the Lawrence Berkeley Laboratory.

How can I measure a voltage of 10^{-15} V? Can I detect the magnetic field generated by the human brain? What is the most sensitive detector of far infrared signals reaching us from distant galaxies? The answers to these seemingly unconnected problems, and to others requiring very sensitive instrumentation, are being provided to an increasing extent by devices based on Josephson junctions (1). These devices offer unprecedented sensitivity in certain applications, and enable us to measure incredibly small signals that are totally inaccessible to other instruments. The Josephson effect is a superconducting phenomenon, and occurs only at temperatures below a few degrees Kelvin. Consequently, until recently operation of Josephson devices was restricted to the low-temperature physics laboratory. However, with the advent of robust and portable cryostats, these instruments are now being used in the field in a variety of applications.

In this article, I will explain the principles of the Josephson effect, describe how practical devices have been made, and discuss some of the applications. I have divided the applications into two broad classes. The first involves the measurement of voltages, magnetic fields, magnetic field gradients, and magnetic susceptibilities at or below audio frequencies (2). In these areas, the Josephson devices have no competitors. The second class is concerned with the detection of high frequency (microwave and far infrared) electromagnetic radiation (2). In this application, the Josephson devices appear to be comparable in performance with other detectors, but improvements are likely to be made in the reasonably near future.

In this short review, I have not been able to even mention a great

deal of elegant and important work in these two areas. I should also point out that there are several other very important applications of the Josephson effect. As I shall describe later, when a Josephson junction is irradiated with microwaves of frequency f, a series of "steps" appears across the junction at voltages $|V_n| = nhf/2e$ (n is an integer, h is Planck's constant, and e is the electronic charge). Parker, Taylor, and Langenberg (3) used this effect to make a very precise measurement of the fundamental constant ratio e/h. Their value differed significantly from the previously accepted value. Taylor et al. (3) subsequently used their value of e/h in a new least-squares adjustment of the fundamental constants. The National Bureau of Standards, and a number of other national laboratories, now use the Josephson voltage-frequency relation to maintain (but not define) the standard of electromotive force (4). The final major application is in computers. The extremely fast switching time and very low dissipation of Josephson junctions make them promising as logic and storage elements for computers (5,6).

Josephson tunneling is a phenomenon of great fundamental physical interest, and has found an amazingly wide variety of applications. Brian Josephson shared the 1973 Nobel Prize in Physics for his prediction of the Josephson Effects.

Superconductivity

In a normal metal, some of the electrons are not bound to the atoms, but able to wander more or less freely through the lattice. It is these free electrons that carry an electric current. The free electrons are scattered by impurities and lattice vibrations (phonons), and a normal metal therefore has a non-zero resistance. At a sufficiently low temperature, typically a few degrees Kelvin, certain metals become superconducting: examples are lead, tin, and niobium. An electric current flows freely through a superconductor without experiencing any resistance. This phenomenon was explained by Bardeen, Cooper, and Schrieffer (7) in a theory for which they were awarded the 1972 Nobel Prize. The basis for their theory is the pairing together of some of the free electrons to form Cooper pairs. These pairs are responsible for carrying the resistanceless current or supercurrent without developing any voltage across the superconductor.

Each pair may be described by a quantum mechanical wave function $\psi(\underset{\sim}{r},t) = |\psi(\underset{\sim}{r},t)|\exp[i\phi(\underset{\sim}{r},t)]$. $|\psi(\underset{\sim}{r},t)|^2$ represents the probability of finding a pair at a point $\underset{\sim}{r}$ at a time t. $\phi(\underset{\sim}{r},t)$ is the phase of the wavefunction. The pair density at any point is found by adding together the contributions from all pairs. In the absence of a current, each pair consists of two electrons of equal and opposite momenta. All pairs therefore have zero momentum. A very important property of a superconductor is that all the pairs are in this same zero momentum state, and have the same value of the phase, ϕ. The absolute phase of the superconductor is not defined, but the relative phase is constant throughout. Thus a

superconductor is said to have phase coherence. The whole collection of pairs may be described by a single macroscopic wavefunction or order parameter $\Psi(\underset{\sim}{r},t) = |\Psi(\underset{\sim}{r},t)|\exp[i\phi(\underset{\sim}{r},t)]$. For this reason, superconductivity is a macroscopic quantum phenomenon: quantum effects are observable on a macroscopic scale.

The concept of phase coherence is central to our understanding of superconductivity, and it has intriguing and unique consequences. One of them is zero resistance. Another is flux quantization. Consider a closed superconducting ring. The total magnetic flux (the product of magnetic field and the area of the ring) enclosed by the ring cannot be arbitrary, but is quantized in units of the flux quantum, $\phi_o = h/2e \simeq 2\times10^{-7}$ G cm^2. The total flux must be equal to $n\phi_o$, where n is an integer. In the presence of an enclosed flux, the phase ϕ of the wavefunction increases uniformly with distance around the ring. The gradient of the phase is proportional to the enclosed flux. In order for $|\Psi|\exp(i\phi)$ to have a unique value at any point, ϕ must change by $2\pi n$ in going once around the ring. It is this requirement that imposes flux quantization.

Suppose we have a superconducting ring in zero magnetic field: the ring is in the n = 0 quantum state. If we apply a magnetic field along the axis of the ring, the ring must remain in the n = 0 state. Consequently, a supercurrent flows around the ring and generates a flux which exactly opposes the applied flux. This supercurrent persists indefinitely, and maintains the n = 0 state. On the other hand, if we cool the ring through its superconducting transition temperature in the presence of a field, the ring will be locked into a quantum state with $n \neq 0$ (in general, a small circulating supercurrent will be required to make the

enclosed flux exactly $n\phi_o$). If the field is removed from the superconducting ring, the ring will remain in the nth quantum state with the creation of a circulating supercurrent that maintains the flux at its initial value. The idea of flux quantization is of great importance in the operation of some of the Josephson devices.

The dc Josephson Effect

A third consequence of phase coherence was first pointed out by Brian Josephson (1) in 1962. He considered two superconductors separated by a thin (10 to 20 Å) insulating barrier, as shown in Fig. 1(a). Above the transition temperature of the superconductors, when the metals are normal, the barrier resistance might be several ohms. However, when the metals are superconducting, Josephson predicted that the barrier resistance would vanish. It would then be possible to pass a small supercurrent through the junction without developing any voltage across the barrier. This process is known as the dc Josephson effect.

The effect involves quantum mechanical tunneling. Cooper pairs are able to "tunnel" from one superconductor to the other through the barrier, retaining their phase coherence in the process. In the absence of any applied fields or currents, the phase is constant throughout the junction. However, if an external current is passed through the junction, there is a phase change $\delta\phi$ across the barrier. The phase change is governed by the external current through the relation (1,8)

$$I = I_c \sin(\delta\phi). \qquad (1)$$

The maximum value of current that can flow as a supercurrent is I_c, known as the critical current. The value of I_c depends upon junction parameters and temperature. If the external current exceeds I_c, the zero-voltage tunneling process ceases, and a voltage appears across the junction.

Practical Josephson Junctions

The Josephson effect was first observed experimentally by Anderson and Rowell (9) in a junction similar to that shown in Fig. 1(b). A strip of tin (for example) is evaporated in a vacuum chamber through a mask on to a glass microscope slide. The strip is oxidized by exposure to the atmosphere, and a second strip of tin evaporated across it. The junction therefore consists of two tin strips separated by an insulating barrier (SIS junction). Leads are connected to the tin strips, and the sample immersed in liquid helium. At temperatures well below the transition temperature of the tin (3.7K), the current-voltage (I-V) characteristic of the junction is similar to that shown in Fig. 1(c). As the current is increased from zero, no voltage appears until the current exceeds the critical current I_c. The voltage then jumps to a non-zero value (dashed line). As the current is increased further, and reduced to zero again, the solid curve is traced out. The critical current may vary from a fraction of a microampère to tens of milliampères.

Other Josephson junctions have been developed and studied. In one variation (10), the oxide barrier of Fig. 1 is replaced by a non-superconducting metal, such as copper (SNS junction). The copper may be 1μm or more in thickness. The Cooper pairs now tunnel through a metal barrier rather than an insulating barrier. This type of junction is particularly

durable. Figure 2(a) shows the Anderson-Dayem bridge (11). The two superconductors are connected by a superconducting bridge of very small cross section. In this structure there is no true tunneling process. Because the bridge is so tiny, the maximum supercurrent it can sustain is relatively small. A related type of structure has been developed and very successfully used by Notarys and Mercereau (12). They "weaken" the bridge by depositing a normal metal on the substrate before the superconductor is evaporated. The bridges are larger, and therefore more durable than the unweakened version. The point contact junction of Silver and Zimmerman (13) [Fig. 2(b)] has been very popular. The junction consists of a sharpened niobium wire pressed against a flat niobium block. The point behaves as a weak link between the wire and the block, although its properties are usually ill-defined. The final type of junction is the SLUG (14). This device consists of a bead of tin-lead solder (a superconductor) frozen on to a length of niobium wire. The solder forms a tight contact around the natural oxide layer of the niobium. However, a continuous junction is not formed, but rather two or three discrete junctions. Figure 2(c) shows idealized I-V characteristic of all the junction types except the tunnel junction. The resistance at currents above the critical current varies from 10^{-6} Ω for junctions with copper barriers to 100 Ω for point contacts. Sometimes there is hysteresis in the characteristic; however, for the device applications, I shall mention it is essential to avoid hysteresis.

The ac Josephson Effect

When there is a voltage across a Josephson junction, the supercurrent

still exists, but oscillates with time. This phenomenon is the ac Josephson effect. The frequency ν of the oscillation is related in a simple way to the voltage V across the junction by the Josephson voltage-frequency relation (1),

$$\nu = \frac{2eV}{h} = \frac{V}{\phi_o} . \qquad (2)$$

As far as we know, this relation is exact. The factor relating frequency and voltage is roughly 484 MHz/μV. The oscillating supercurrents persist for voltages of up to at least several millivolts and frequencies in excess of 10^{12} Hz. All of the junctions described earlier exhibit the ac Josephson effect.

Cryogenics

In the first sections, I have tried to give some feeling for the basic ideas of Josephson tunneling. Before I describe their application to devices, I shall first briefly mention the necessary cryogenic systems. The devices are usually operated at 4.2K, the boiling point of liquid helium under atmospheric pressure. The junctions are often immersed in the liquid. However, the boiling of the liquid helium sometimes generates excess noise, and for the most sensitive measurements, it may be necessary to mount the device inside a can which is surrounded by the liquid. The traditional low temperature cryostat consists of a double-walled glass dewar containing liquid helium, surrounded by a second dewar containing liquid nitrogen. This cryostat is somewhat cumbersome and fragile for use in the field, and more compact and robust

versions have been developed. These cryostats are of metal or fiberglass. The fiberglass dewar is non-magnetic, an important consideration in the measurement of external magnetic fields. The liquid helium is contained in an inner vessel suspended inside a larger evacuated container. A cooled thermal radiation shield between the two vessels reduces the heat load due to thermal radiation. A typical cryostat can hold one charge of liquid helium for several days, consuming as little as one liter per day.

SQUIDS

The basic detector for low frequency measurements is the SQUID (Superconducting Quantum Interference Device). The SQUID combines flux quantization and Josephson tunneling. There are two types, the dc SQUID and the rf SQUID.

In the dc SQUID, two Josephson junctions are mounted on a superconducting ring [Fig. 3(a)]. The I-V characteristic (which must be non-hysteretic) is similar to that of a single junction. However, if a magnetic field is applied along the axis of the ring, the combined critical current oscillates as the field is increased. The period of the oscillations is the flux quantum, ϕ_o [Fig. 3(b)]. This periodic behavior reflects the macroscopic quantum nature of the SQUID, and was first observed by Jaklevic et al. (15). As the external flux is steadily increased from zero, the SQUID does not remain in its initial quantum state. Instead, it makes transitions to higher states: for example, from the nth state to the (n+1)th state when the applied flux is $(n+1/2)\phi_o$. As a result, the circulating current in the SQUID is periodic in the

applied flux, the period again being ϕ_o (in the case of a superconducting ring, the circulating current would increase linearly with the applied flux, and the quantum state would not change.) The circulating current is zero whenever the applied flux is $n\phi_o$, and a maximum whenever it is $(n+1/2)\phi_o$. The presence of the circulating current reduces the critical current of the SQUID. The critical current is therefore a maximum when the applied flux is $n\phi_o$, and a minimum whenever it is $(n+1/2)\phi_o$.

In a practical application, the junctions are biased at a non-zero voltage by a constant current I_o, which always exceeds the critical current [Fig. 3(c)]. Thus the voltage across the SQUID oscillates as a function of applied field. Changes in this voltage are amplified by conventional room-temperature electronics.

The SLUG is also a dc SQUID. The critical current of the SLUG oscillates as a function of the current in the niobium wire on which the solder bead is formed. This behavior indicates that only two (or perhaps three or four) junctions are formed between the wire and the solder. The magnetic flux generated by the current in the niobium wire modulates the critical current.

The rf SQUID was developed by Zimmerman and co-workers (16) and Mercereau and co-workers (17). It consists of a single Josephson junction mounted on a superconducting ring (Fig. 4). A steadily increasing magnetic field again induces quantum transitions in the SQUID. There is therefore a circulating supercurrent that is periodic in the applied flux, with a period ϕ_o. This current is detected by coupling the SQUID to the inductance of a resonant LC circuit [Fig. (4)]. An alternating current at the resonant frequency (typically 30 MHz) generates an

alternating voltage across the resonant circuit. The amplitude of this rf voltage depends on the value of the circulating supercurrent in the SQUID, and is therefore periodic in the flux applied to the SQUID. The rf voltage is amplified and rectified by conventional electronics.

Both the dc and rf SQUIDs produce a voltage that is periodic in the flux applied to them, with a period ϕ_o. SQUIDs are digital magnetometers: One has only to count the oscillations in voltage to measure the size of the applied field. However, in practice they are almost never used in a digital mode. Instead they are incorporated in a feedback circuit, the whole system producing a voltage output that is linearly proportional to the applied flux. The principle is illustrated in Fig. (5) for a dc SQUID.

The SQUID is biased with a current I_o as described earlier. The voltage appearing across the SQUID is amplified by conventional electronics. The output from the amplifier is fed via a resistance R_F into a coil L_F which is coupled to the SQUID. Suppose a small field δH is applied to the SQUID. The change in the SQUID voltage is amplified and fed back as a current I_F into the coil L_F. The flux produced by this current opposes and exactly cancels δH. The total flux threading the SQUID is therefore zero, and the output voltage $V_o = I_F R_F$ is linearly proportional to δH. The SQUID is thus the null detector in a feedback system.

Exactly the same principle is used in the operation of the rf SQUID. (In both cases, in practice the electronic readout from the SQUID is a little more complicated.) The performances of the dc and rf SQUIDs are comparable. Either type of SQUID may be used in the applications that follow. In the linearized mode, the resolution of a SQUID is a fraction of a flux quantum. A good system will resolve 10^{-4} ϕ_o in a bandwidth of 1 Hz ($10^{-4}\phi_o/\sqrt{Hz}$). The

frequency response is from zero up to typically a few kHz. It is intriguing to realize that this sensitivity represents the detection of a very small amount of energy. The change in magnetic field energy δE arising from a flux $\delta\phi$ is $(\delta\phi)^2/2L$, where L is the inductance of the SQUID. If $\delta\phi = 10^{-4}\ \phi_o \approx 2 \times 10^{-11}$ G cm$^2 \approx 2 \times 10^{-19}$ Wb, and $L \approx 10^{-9}$ H, we find that $\delta E \approx 2 \times 10^{-29}$ J.

The area of a SQUID is typically 10^{-2} cm^2. The resolution in magnetic field is therefore roughly 10^{-9} G/$\sqrt{\text{Hz}}$. In order to take advantage of this high sensitivity, it is essential to shield the SQUID against fluctuations in the earth's magnetic field, typically 10^{-5} G over a period of 1 sec. This shielding is achieved by enclosing the SQUID in a superconducting can. The can does not reduce the external field to zero, but "freezes in" a constant field.

Two typical SQUIDs and a SLUG are shown in Fig. 6. The rf SQUID shown contains a double loop with a point-contact across the narrow region. This device was originally developed by Zimmerman et al.(16), and is now available commercially from SHE Corporation. The dc SQUID and the SLUG are from my own laboratory. A further type of rf SQUID (not shown) has been developed by Mercereau and Nisenoff (17). A thin ring of superconducting film is evaporated on to a quartz rod, and a constriction etched or cut into the ring. This type of SQUID is also commercially available. Although point-contact devices have been very widely used, it is probable that they will ultimately be replaced by thin film devices, which are more stable. The dc SQUID preceded the rf SQUID, and was and is used successfully. However, present trends favor the rf SQUID, which involves only a single junction, and which is

available commercially.

Flux Transformer

The superconducting flux transformer, shown schematically in Fig. 7(a), is used in almost all measurements of magnetic field. The transformer is entirely superconducting, and consists of a pick-up loop (primary coil), and a secondary coil tightly coupled to a SQUID. The SQUID and secondary are enclosed in a superconducting can. A magnetic field applied to the pick-up loop generates a persistent current, which in turn induces a flux in the SQUID. The sensitivity of the SQUID can be appreciably enhanced by proper transformer design, and resolutions of better than 10^{-10} $G/\sqrt{Hz}$ have been achieved.

However, this high sensitivity is of limited use in an unshielded environment because of the noise in the earth's field. Of far greater practical importance is the magnetic field gradiometer, illustrated in Fig. 7(b). In this configuration, the transformer has two pick-up coils of equal area. They are arranged so that a uniform magnetic field does not induce a supercurrent. If the field has a gradient (for example, $\partial H_z/\partial x$), the fields applied to the two coils will differ, and the induced supercurrent will be proportional to the difference. The SQUID system thus measures a gradient. The gradiometer can be made in many configurations: gradiometers measuring $\partial H_z/\partial z$ are commonly used, and higher derivatives could, in principle, also be measured. The first published account of a gradiometer appears to be that of Zimmerman and Frederick (18), who reported a resolution of 10^{-10} $G/cm/\sqrt{Hz}$. Sensitivities at least an order of magnitude higher have been subsequently achieved.

The great advantage of a gradiometer is that it discriminates against signals generated a large distance away in favor of signals generated locally. Apart from man-made interference, the main sources of magnetic noise are disturbances in the upper atmosphere, and fluctuations in the earth's field. Both sources are relatively distant, so that although their fields at the detector may be large, their field gradients are small. Suppose that we are concerned with measuring a small magnetic signal from a nearby source. Although its field amplitude may be below the ambient field noise, its gradient amplitude may be considerably above the ambient gradient noise. In the same way, the gradient produced by a source a few centimeters away may exceed the gradient noise generated by a passing automobile or a power line tens of meters away. For these reasons, most of the practical devices for use in an open environment are likely to be gradiometers.

Apart from measurements in the physics laboratory, there appear to be several other important applications of magnetometers and gradiometers. Cohen et al. (19) have pioneered the use of superconducting devices in magnetocardiography, using a magnetometer in a magnetically screened room. In one study, Cohen and McCaughan obtained magnetocardiograms at various points on the torso of a patient. Their results are shown in Fig. 8. The outline of the heart is shown dotted. The signals obtained at different points clearly differ substantially. The peak-to-peak signal amplitude is about 5×10^{-7} G, much greater than the background noise. At present, it is not known how to interpret the differences in these signals. However, it is to be hoped that intensive clinical studies will eventually enable one to obtain a more precise diagnosis than is possible from electrocardiograms. In clinical practice, one would take magneto-

cardiograms with a gradiometer, so that a shielded room would be unnecessary(18).

Dr. Cohen has also detected alpha-waves from the brain magnetically. The signal amplitude is smaller than that developed by the heart, perhaps 10^{-9} G. It seems likely that magnetoencephalography would require both patient and detector to be in a magnetically shielded room to reduce the background noise to an acceptable level. Again, this application has exciting possibilities, but extensive clinical studies are obviously needed.

Magnetometers and gradiometers have considerable potential in geophysics. For example, it might be possible to search for mineral deposits by means of gradient surveys. Morrison at the University of California at Berkeley is investigating an alternative surveying technique. He applies an electric current pulse between two probes in the ground a few hundred meters apart. The induced polarization is characteristic of the rocks through which the current flows, and is detected by a SQUID magnetometer. Another intriguing possibility is in the prediction of earthquakes or volcanic eruptions. There is evidence to suggest that over periods of a few days prior to an earthquake, there are magnetic disturbances along the fault line. Such disturbances were observed by Moore just before the 1964 Alaskan earthquake (20). Similar effects were observed by Johnston and Stacey before the eruption of Mount Ruapehu, New Zealand, in 1968 (21). The physical origin of these disturbances is not firmly established. However, a likely cause is piezomagnetism, that is, the magnetization of a body under stress. All of the data so far have been collected with

magnetometers: a magnetometer near the disturbance is compared with one placed some distance away (typically 10 km). This procedure minimizes noise due to distant fluctuations, for example, in the ionosphere. It would obviously be of some interest to observe changes in the magnetic field gradient near a fault or a volcano. The gradiometer would of course discriminate against distant noise in favor of more local signals. To my knowledge, no such observations have yet been made.

I should also like to mention the use of SQUIDs to measure magnetic susceptibility, that is, the ratio of magnetization to applied magnetic field. The sample is inserted into one loop of a gradiometer (Fig. 7(b)), and a uniform magnetic field applied to both loops. If the sample has a non-zero susceptibility, it will change the magnetic flux threading the loop in which it is placed. The SQUID output will be proportional to the susceptibility. Careful shielding against external field fluctuations is essential. In this way, Mercereau and co-workers have measured the susceptibility of biochemical samples over a temperature range from 4K to 300K (22). A related application is the measurement of susceptibility of rock samples. Day has taken nuclear magnetic resonance curves in a similar manner (23). In all of these measurements, the high sensitivity of the SQUID enables one to use minute samples, an important consideration, especially in biological work.

Voltmeter

A SQUID or SLUG can be used readily as a voltmeter. In Fig. 7(c), a resistance R is in series with the superconducting coil coupled to a SQUID. Alternatively, the resistance may be connected to the niobium wire

on which a SLUG has been made (Fig. 6). In either case, a signal voltage V_s applied to the terminals generates a current $I_s = V_s/R$ that is detected by the superconducting device. These voltmeters have been widely used in solid state physics to measure tiny voltages. The sensitivity is very great, and voltages as low as 10^{-15} $V/\sqrt{Hz}$ can be detected routinely. The resolution is often limited by the Johnson noise generated in the series resistance or the source resistance: the Johnson noise in 10^{-8} Ω at 1K is about 10^{-15} $V/\sqrt{Hz}$. This fact has been utilized by Giffard, Webb, and Wheatley (24) in their noise thermometer. The terminals marked V_s in Fig. 7(c) are shorted together, so that the circuit consists of a superconducting loop containing a resistance R. The mean square Johnson noise current is proportional to the absolute temperature, and is measured by the SQUID in the usual way. Giffard et al. were able to measure temperatures down to a few mK with this technique.

Effect of Microwaves on Josephson Junctions

I will briefly discuss the effect of high frequency (microwave and far infrared) radiation on Josephson junctions (25). If microwaves of a single frequency f are coupled to a Josephson junction, for example a point contact, the I-V characteristic is modified as shown in Fig. 9. A series of current steps is induced, the voltage along each step being constant. The steps appear at voltages

$$|V_n| = nhf/2e, \tag{3}$$

where n is an integer. The height of the steps oscillates as the microwave

power is increased. The detailed theory of the behavior of a junction in a microwave field is complicated. The essential point is that the microwaves at frequency f beat in the non-linear junction with the ac Josephson currents whose frequency ν depends upon the voltage across the junction. Whenever $(\nu \pm nf) = 0$, there is a zero-frequency beat, which is manifested as a current step. A simple quantum description of the effect has been given by Josephson (1). When the junction is biased at a voltage V, the energy difference between Cooper pairs on opposite sides of the barrier is just 2eV. Whenever this energy difference is exactly nhf, pairs can cross the barrier coherently with the emission or absorption of n microwave photons.

Josephson junctions can be used as detectors of electromagnetic radiation in a number of different ways. I have decided to discuss just two of these methods which seem to me the most promising. The devices concerned are the broadband square law detector and the heterodyne linear detector. I should emphasize that there is considerable work in progress in this field, and that it is not yet entirely clear which devices will ultimately have the best performance. In any case, different applications may be better suited by different modes of operation.

Square Law Broadband Detector

The use of a Josephson junction as a broadband detector was first investigated by Grimes, Richards, and Shapiro (26). When microwaves

generate constant current steps, at the same time they reduce the magnitude of the critical current. In fact, the critical current is also an oscillatory function of the microwave field. The critical current corresponds to the n = 0 induced step. Suppose one applies broadband radiation (that is, radiation containing a wide range of frequencies) to a junction. The steps on the I-V characteristic will be blurred out, and no discrete steps will be visible. However, the critical current responds to each frequency component of the radiation, and will be correspondingly modified. (Equation (3) is satisfied for n = 0 by all values of frequency f.) The critical current does not respond uniformly to all frequencies, the response becoming less sensitive as the frequency increases. It can be shown that for small signal levels,

$$\Delta I_c \propto V_s^2/\omega_s^2, \tag{4}$$

where V_s is the voltage induced across the junction by radiation at a frequency ω_s, and ΔI_c is the resulting depression in the critical current. The fact that ΔI_c is proportional to V_s^2 implies that the junction is a square law detector, and that it responds to the power rather than the amplitude of the radiation.

All successful detectors have used point-contact junctions. It appears that the point-contact couples more efficiently to the radiation than other types of junction, although the coupling properties of Anderson-Dayem bridges (11) are now being extensively studied. The point-contact is mounted transversely across a waveguide or light pipe (oversized waveguide) so that the electric field of the incoming radiation

generates currents through the junction. The waveguide is usually terminated by a movable plunger which is adjusted to maximize the coupling efficiency. Changes in the critical current in response to radiation are detected by a method identical to that used for the dc SQUID [Fig. 3(c)]. A constant current I_o biases the junction at a non-zero voltage. When the critical current changes, the I-V characteristic and hence the voltage across the junction are modified. Since the detector responds to a wide range of frequencies, the bandwidth is often restricted externally to a narrow range about some central frequency (for example, by an interferometer). One sweeps the central frequency to obtain the spectrum of the radiation. It is usual to chop the incoming radiation at a few tens of Hz, and to detect the resulting ac signal that appears across the junction.

The most important frequency range for the Josephson detector is in the far infrared, around 300 GHz (1 mm wavelength). Competing detectors at these frequencies are relatively less sensitive that those available in the microwave or infrared regions. Apart from laboratory experiments, the most significant application of these detectors appears to be in far-infrared astronomy. Ulrich has used a point-contact detector for astronomical observations at the McDonald Observatory at the University of Texas. He estimates the sensitivity of his detector to be about 10^{-14} W/$\sqrt{\text{Hz}}$ at 1 mm. This figure is comparable with the sensitivity of the best semiconducting broadband bolometers (27).

Heterodyne Detector

In the heterodyne detector, the signal to be detected is combined (mixed) with the output from a local oscillator in the non-linear Josephson junction. In the simplest case, the signal frequency, f_s, is close to the local oscillator frequency, f_{LO}. The amplitude of the local oscillator output is much greater than the signal amplitude. Under these conditions, the signal and local oscillator output mix in a relatively simple way, as indicated in the phasor diagram of Fig. 10(a). The local oscillator output is represented by a vector of length A_{LO} rotating at an angular frequency $\omega_{LO} = 2\pi f_{LO}$. To this vector is added the signal vector, of length A_s, rotating at a frequency ω_s. Relative to the local oscillator vector, the signal vector rotates at a frequency $\omega_I = |\omega_{LO}-\omega_s|$ (the intermediate frequency), which is much less than either ω_{LO} or ω_s. The resultant vector A therefore rotates with a frequency ω_{LO}, but its amplitude is modulated at a frequency ω_I between the limits $A_{LO} + A_s$ and $A_{LO} - A_s$.

The effect of this mixing process on the Josephson junction can be readily understood. In the absence of a signal, the large local oscillator output induces a series of steps in the I-V characteristic, as shown in Fig. 9. When the signal is applied, the effect of the local oscillator on the junction is modulated at a frequency $f_I = |f_{LO}-f_s|$. Consequently, the whole I-V characteristic is modulated at f_I, as shown in Fig. 10(b). A constant current I_o biases the junction at a voltage roughly one half that of the n = 1 step. In the presence of a signal, the voltage across the junction oscillates at a frequency f_I, and

with an amplitude that is proportional to the signal amplitude. This voltage is amplified by an intermediate frequency amplifier, and subsequently measured.

The best characterized Josephson heterodyne detector at present appears to be that of Taur, Claassen, and Richards at Berkeley (28). They used a point contact device, mounted in the way described for the broadband detector. The local oscillator frequency was 36 GHz. Taur et al. chose this relatively low frequency to enable them to make a thorough study of the properties of the detector. Eventually, it should be possible to operate the detector at 300 GHz. It is a little difficult to assess just how well the device will perform at this frequency. If the performance extrapolates in the expected way, the Josephson heterodyne detector is likely to be the most sensitive available for some applications. However, the performances of the Josephson detectors and of competing detectors (25) are steadily improving, and it is not clear which of them will eventually have the highest resolution. I can probably best sum up the heterodyne detectors by saying that the Josephson devices are at least holding their own in a rapidly changing field, but that much work remains to be done.

Josephson Junction Broadband Bolometer

Hoffer, Richards and I (29) have developed a bolometer that employs a Josephson junction in a quite different way from methods previously described. A bolometer consists of a small piece of material of heat capacity C suspended inside a vacuum can by a thermal link of conductance K. When electromagnetic radiation of power ΔP is absorbed by the bolometer,

its temperature is increased by $\Delta T = \Delta P/K$. If we measure the change in some temperature-sensitive parameter of the bolometer, we can estimate ΔT and thus ΔP. The response time of the bolometer is C/K. It is necessary to make K small to achieve high sensitivity. Therefore C should be small to keep the response time down to a reasonable level.

Figure 11 is a photograph of our bolometer. It consists of a sapphire substrate (of low heat capacity) suspended by two nylon threads. A Pb-Cu-Pb (SNS) Josephson junction is evaporated on to the sapphire. The critical current of this junction increases exponentially as the temperature is lowered. Hence a small change in the temperature of the substrate produces a substantial change in the critical current. Electrical connection is made to the SNS junction by evaporating lead on to the edges of the substrate and onto the two nylon threads on the left hand side of the photograph. A heater is mounted next to the SNS junction for calibration purposes, and is connected to the two right-hand lead-coated threads. The rear of the substrate is coated with a thin film of bismuth to couple the bolometer to the incoming electromagnetic radiation. The whole device is mounted in a vacuum can which is immersed in liquid helium. A SQUID detects changes in the critical current of the SNS junction.

The bolometer was tested by determining the smallest power in the heater that could be detected. The best sensitivity that we have achieved to date is 4×10^{-15} W/$\sqrt{\text{Hz}}$. We feel that the ultimate sensitivity of the bolometer is about 10^{-15} W/$\sqrt{\text{Hz}}$. We have also made preliminary measurements on the absorptivity of the bismuth-coated sapphire substrate, and found that it absorbs strongly over a range of wavelengths from

0.1 mm to a few mm. It therefore seems probable that this bolometer will have a sensitivity approaching 10^{-15} W/$\sqrt{\text{Hz}}$ at wavelengths around 1 mm. This resolution would make it the most sensitive broadband detector available.

Summary

Josephson tunneling is a phenomenon of very great fundamental physical interest, and also of diverse and far reaching application. We have already seen a very precise measurement of e/h which has had considerable impact on the values of many of the fundamental constants (4). The NBS now maintains the standard volt in terms of a Josephson frequency. The use of Josephson junctions in computers offers the possibilities of increased speed and reduced size. SQUIDs, coupled with flux transformers, give us unprecedented resolution in the measurement of low frequency voltages, and magnetic fields, field gradients, and susceptibilities. This particular area is presently one of rapid growth, largely because of the availability of SQUIDs commercially. Thus scientists previously unconnected with low temperature physics are now able to take advantage of the great sensitivity of SQUIDs. It seems very likely that these devices will be used in other fields to an increasing extent. Finally, the Josephson junction has considerable promise as a broadband detector and as a heterodyne detector in the far infrared.

References and Notes

1. B. D. Josephson, Phys. Letters 1, 251, (1962); Advances in Physics 14, 419 (1965).
2. A detailed review of the low frequency applications has been given by J. Clarke, Proc. IEEE 61, 8 (1973); and of the high frequency detectors by P. L. Richards, F. Auracher, and T. Van Duzer, ibid., 61, 36 (1973).
3. D. N. Langenberg, W.H. Parker, and B.N. Taylor, Phys. Rev. 150, 186 (1966). B.N. Taylor, W.H. Parker, and D.N. Langenberg, Rev. Mod. Phys. 41, 375 (1969).
4. B.N. Taylor, W.H. Parker, D.N. Langenberg, and A. Denenstein, Metrologia 3, 89 (1967).
5. J. Matisoo, Proc. IEEE 55, 172 (1967).
6. T. A. Fulton, R. C. Dynes, and P. W. Anderson, Proc. IEEE 61, 28 (1973).
7. J. Bardeen, L. N. Cooper, and J. R. Schrieffer, Phys. Rev. 108, 1175 (1957).
8. P. W. Anderson, in Lectures on the Many Body Problem, Ravello, 1963, (ed. E. R. Caianiello, Academic Press, New York, 1964).
9. P. W. Anderson and J. M. Rowell, Phys. Rev. Lett. 10, 230 (1963).
10. J. Clarke, Proc. Roy. Soc. (London) A308, 447 (1969).
11. P. W. Anderson and A. H. Dayem, Phys. Rev. Lett. 13, 195 (1964).
12. H. A. Notarys and J. E. Mercereau, in Proc. Intern. Conf. on the Science of Superconductivity, Stanford, 1969 (North-Holland, 1971), p. 424; J. Appl. Phys. 44, 1821 (1973).
13. J. E. Zimmerman and A. H. Silver, Phys. Rev. 141, 367 (1966).
14. J. Clarke, Phil. Mag. 13, 115 (1966).
15. R. C. Jaklevic, J. Lambe, A. H. Silver, and J. E. Mercereau, Phys. Rev. Lett. 12, 159 (1964).
16. J. E. Zimmerman, P. Thiene, and J. T. Harding, J. Appl. Phys. 41, 1572 (1970).

17. J. E. Mercereau, Rev. de Phys. Appl. 5, 13 (1970); M. Nisenoff, ibid. 5, 21 (1970).

18. J. E. Zimmerman and N. V. Frederick, Appl. Phys. Letters 19, 16 (1971).

19. D. Cohen, E. A. Edelsack, and J. E. Zimmerman, Appl. Phys. Letters 16, 278 (1970); D. Cohen and D. McCaughan, Amer. J. Cardiology, 29, 678 (1972)

20. G. W. Moore, Nature 203, 508 (1964).

21. M. J. S. Johnston and F. D. Stacey, Nature 224, 1289 (1969).

22. H. E. Hoenig, R. H. Wang, G. R. Rossman, and J. E. Mercereau, in Proc. 1972 Appl. Superconductivity Conf. Annapolis, Maryland, p. 570.

23. P. E. Day, Phys. Rev. Letters 29, 540 (1972).

24. R. P. Giffard, R. A. Webb, and J. C. Wheatley, J. Low Temp. Phys. 6, 533 (1972).

25. S. Shapiro, Phys. Rev. Letters 11, 80 (1963).

26. C. C. Grimes, P. L. Richards, and S. Shapiro, Phys. Rev. Letters 17, 431 (1966); J. Appl. Phys. 39, 3905 (1968).

27. For a recent review of the sensitivity of various detectors, see A. Penzias, to be published in Proc. Intern. Conf. on "Detection and Emission of Electromagnetic Radiation with Josephson Junctions", Perros-Guirec, France, 1973.

28. Y. Taur, J. H. Claassen, and P. L. Richards, ibid.

29. J. Clarke, G. I. Hoffer, and P. L. Richards, ibid.

30. I thank Professor P.L. Richards, Dr. J.H. Claassen and Mr. Y. Taur for discussion of far infrared detectors, Professor Bhattacharyya, Dr. M.J.S. Johnston, and Professor H.F. Morrison for discussion of geophysical measurements, and Dr. D. Cohen for discussion on

magnetocardiology, and for supplying Fig. 8, which was originally published in Amer. J. Cardiology, 29, 678 (1972). This work was supported in part by the U.S.A.E.C.

Figure Captions

Fig. 1 (a) Idealized Josephson junction; (b) superconductor-insulator-superconductor tunnel junction; (c) current-voltage (I-V) characteristic of tunnel junction.

Fig. 2 (a) Anderson-Dayem Bridge evaporated on substrate; (b) point contact; (c) idealized I-V characteristic of SNS junction, Dayem bridge, Notarys-Mercereau bridge, point-contact, or SLUG.

Fig. 3 (a) Dc SQUID: two Josephson junctions (X) on a superconducting ring; (b) oscillations in critical current, as a function of applied flux; (c) when the applied flux changes from an integral number of flux quanta to a half-integral number, the voltage across the dc SQUID changes by δV.

Fig. 4 Rf SQUID: a single junction (X) on a superconducting ring. The ring is coupled to an LC resonant circuit to which an rf current $i_o \sin \omega t$ is applied. The amplitude of the voltage across the resonant circuit, v_o, is an oscillatory function of the flux applied to the SQUID.

Fig. 5 Feedback circuit for dc SQUID.

Fig. 6 The upper device is an rf SQUID. The device on the lower left is a SLUG, and that on the lower right is a dc SQUID.

Fig. 7 (a) Flux transformer; (b) gradiometer; (c) voltmeter.

Fig. 8 Magnetocardiograms taken by Cohen and McCaughan at various points outside the torso of a male patient. The dotted outline represents the position of the heart.

Fig. 9 I-V characteristic of point contact irradiated with microwaves at 4 GHz.

Fig. 10 Heterodyne detector: (a) phasor diagram, showing addition of A_{LO}, which has a frequency ω_{LO}, and A_s, which has a frequency ω_s. If $\omega_{LO} \approx \omega_s$, the resultant vector A is amplitude modulated at a frequency $\omega_I = |\omega_{LO} - \omega_s|$. (b) The solid line (———) shows the effect of the local oscillator on the I-V characteristic. An applied signal modulates the characteristic between the limits set by the dotted lines (- - - - - - - - -). I_o(— — — —) is a constant current bias.

Fig. 11 SNS bolometer.

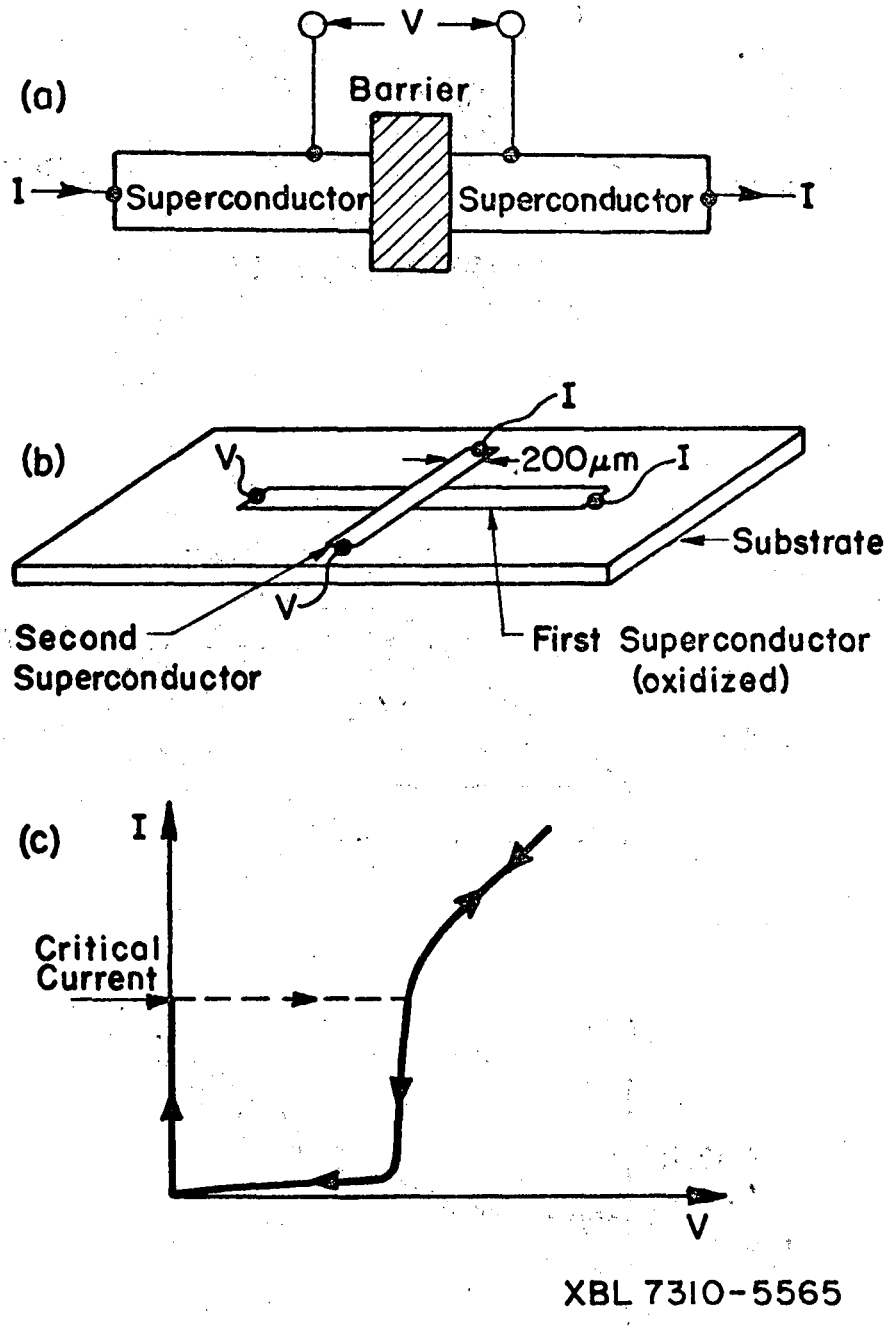
(a)
V
Barrier
I
Superconductor
Superconductor
I
(b)
I
V
200μm
I
Substrate
V
Second
Superconductor
First Superconductor
(oxidized)
(c)
I
Critical
Current
V
XBL 7310-5565

Fig. 1

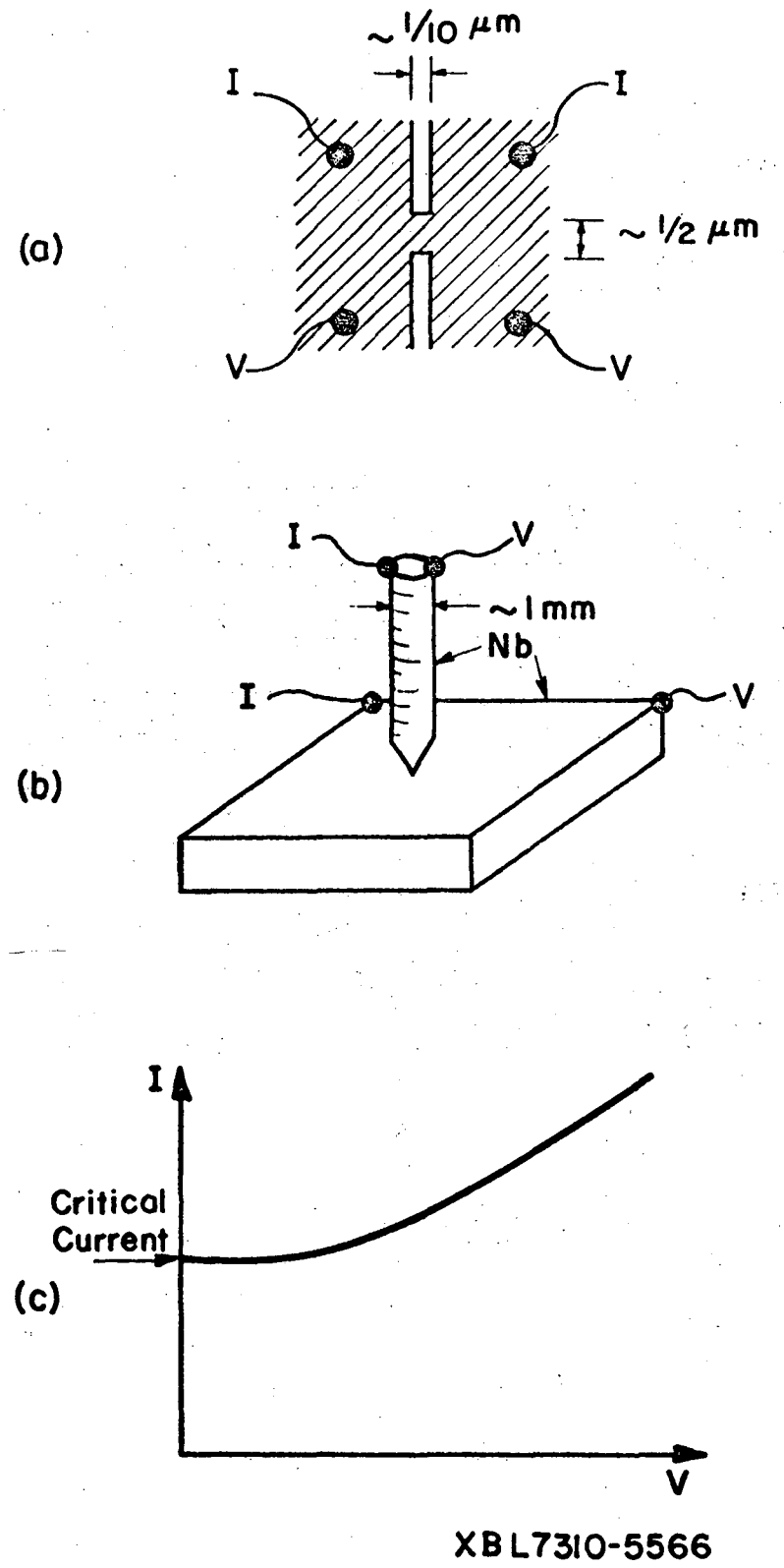
~ 1/10 μm
I
I
~ 1/2 μm
(a)
V
V
I
V
~1mm
Nb
I
V
(b)
I
Critical
Current
(c)
V
XBL7310-5566

Fig. 2

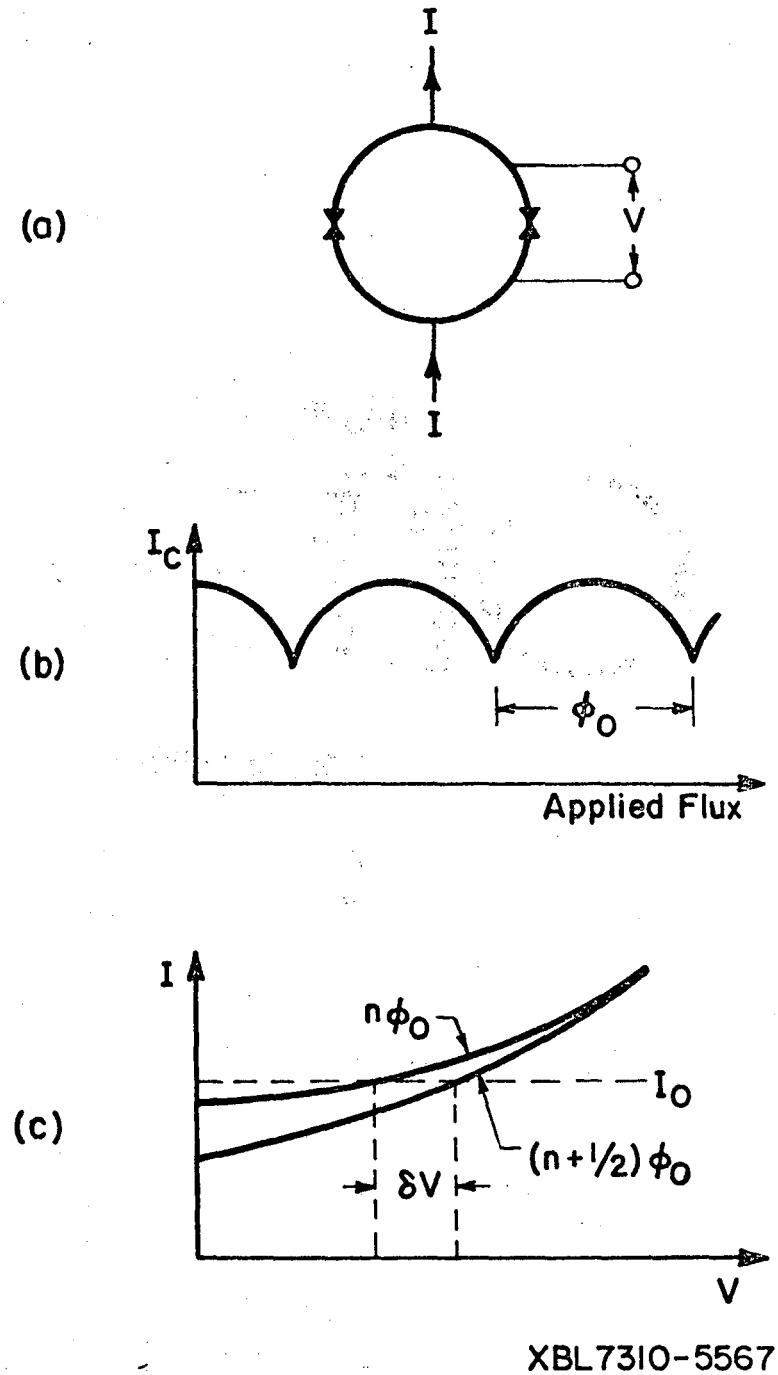
(a)
I
V
I
(b)
I_c
ϕ_o
Applied Flux
(c)
I
$n\phi_o$
I_o
$(n+1/2)\phi_o$
δV
V
XBL7310-5567

Fig. 3

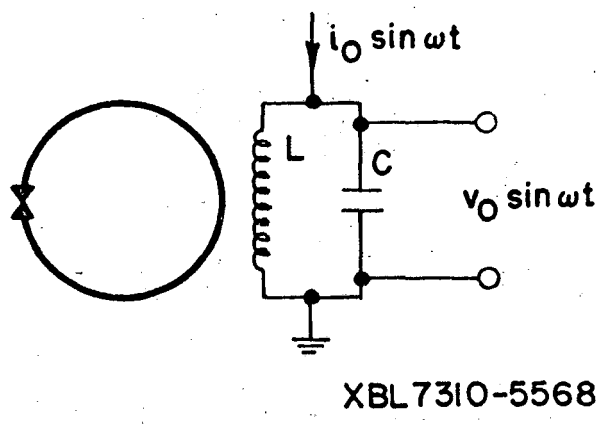

Fig. 4

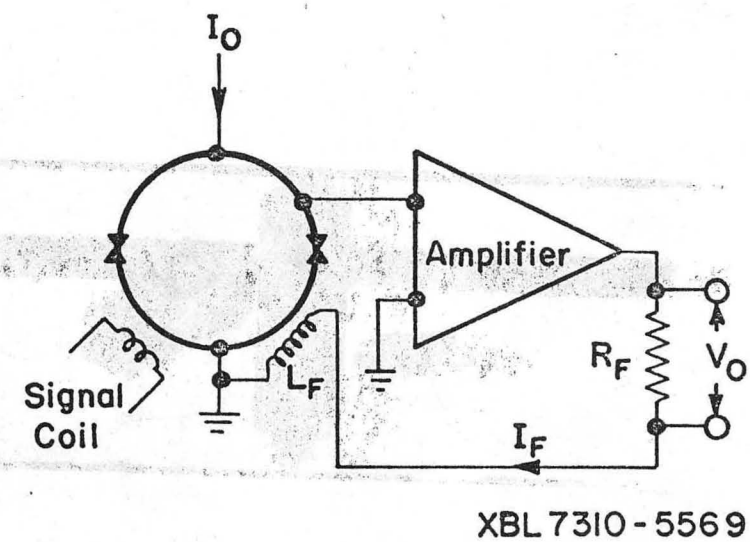

Fig. 5

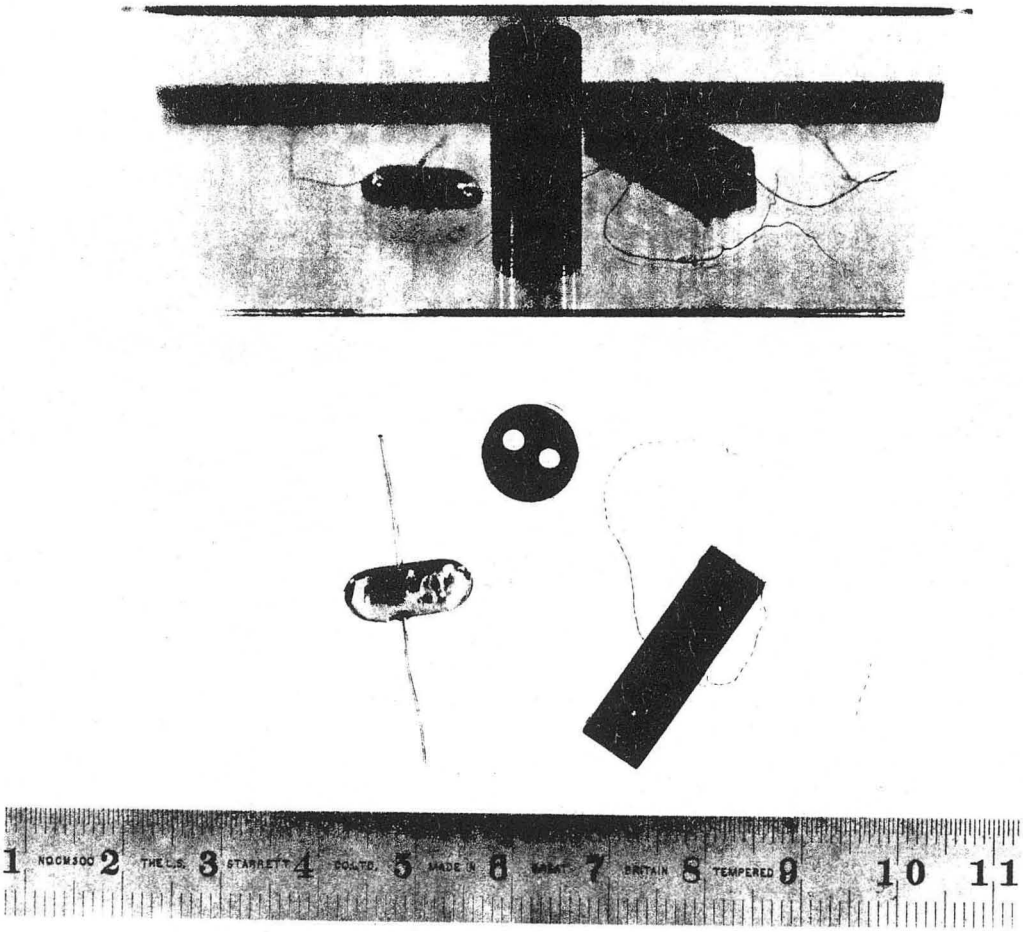

Fig. 6

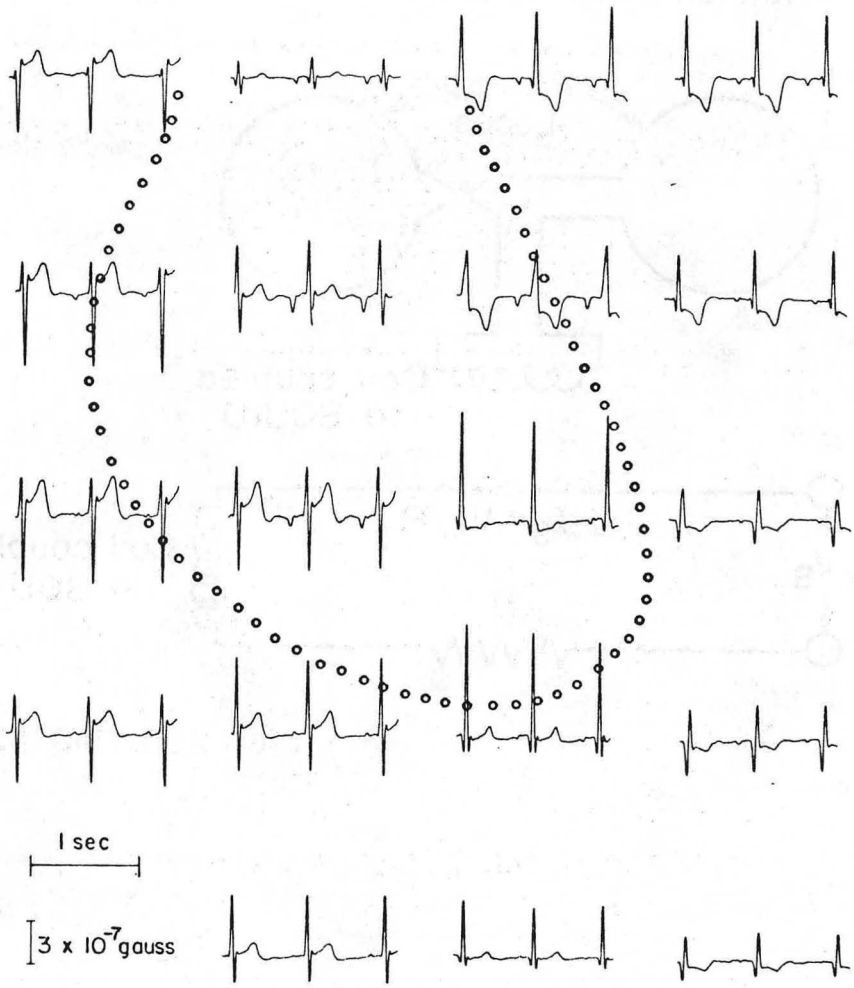

Fig. 8

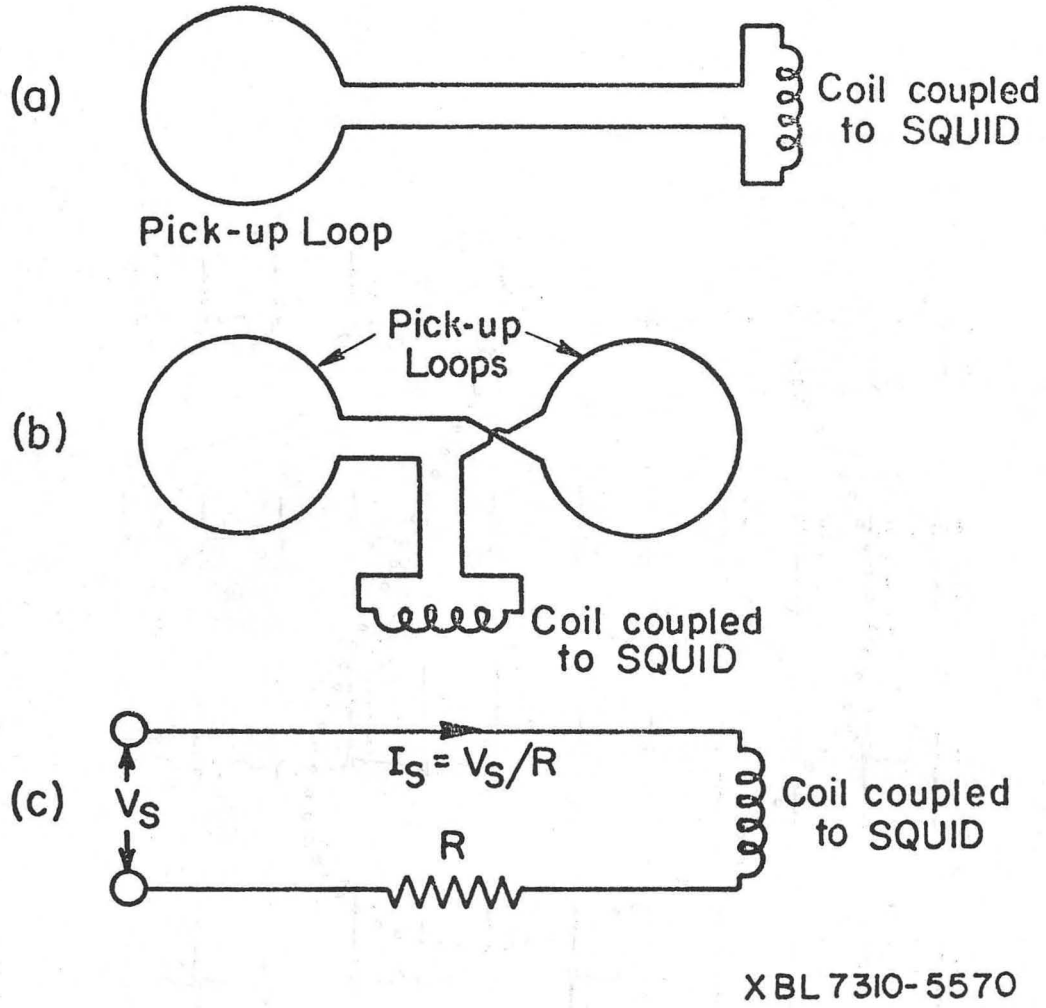
(a)
Coil coupled to SQUID
Pick-up Loop
(b)
Pick-up Loops
Coil coupled to SQUID
(c)
V_S
$I_S = V_S/R$
R
Coil coupled to SQUID
XBL 7310-5570

Fig. 7

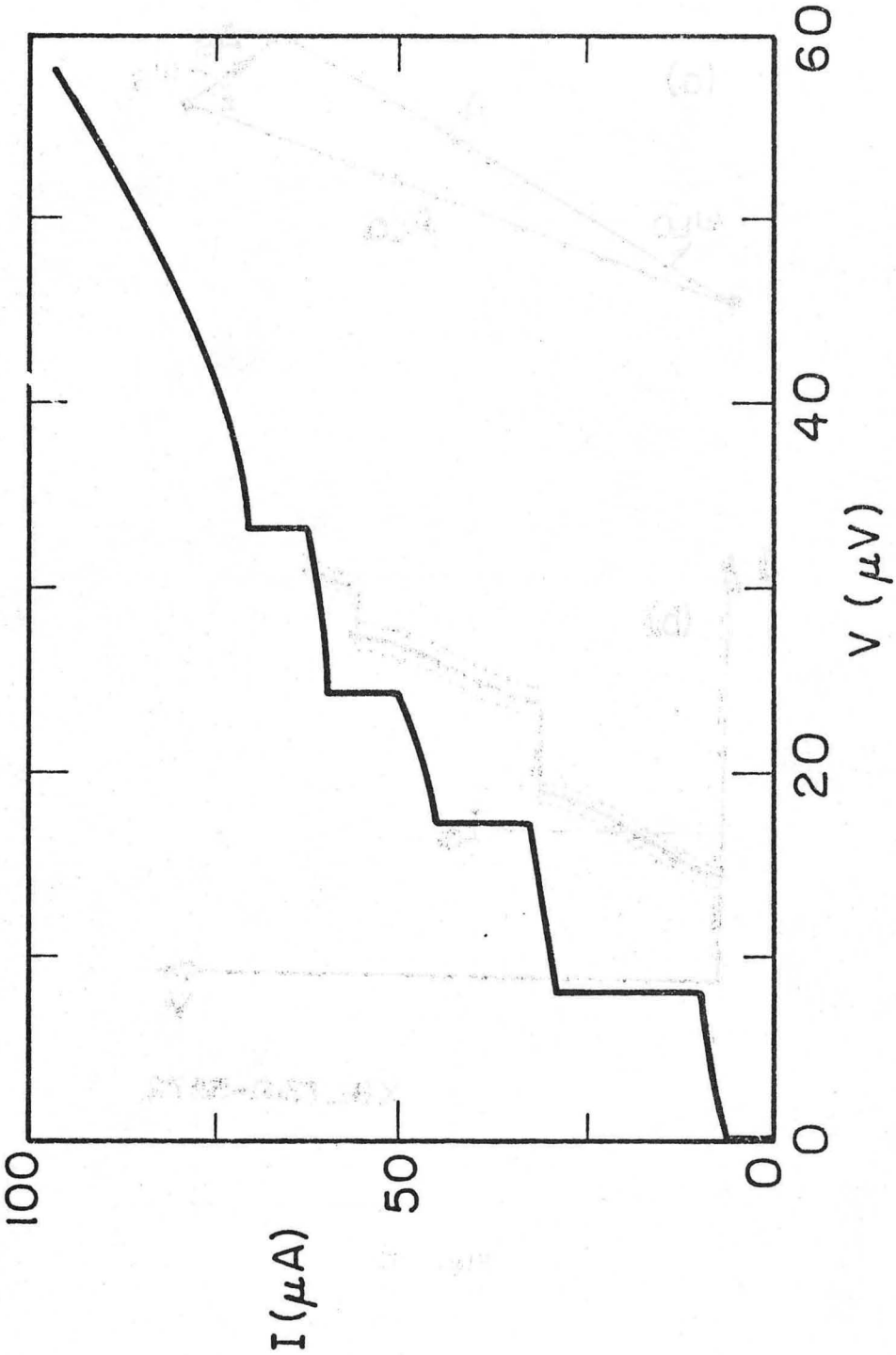

XBL 7310-5571

Fig. 9

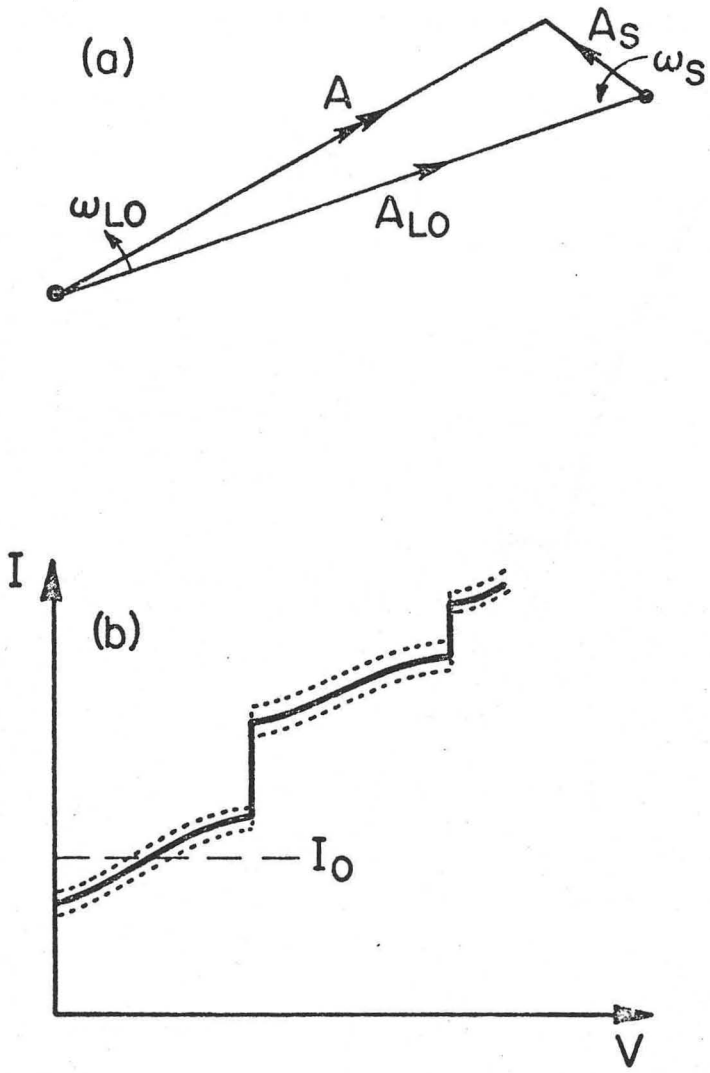

XBL 7310-5572

Fig. 10

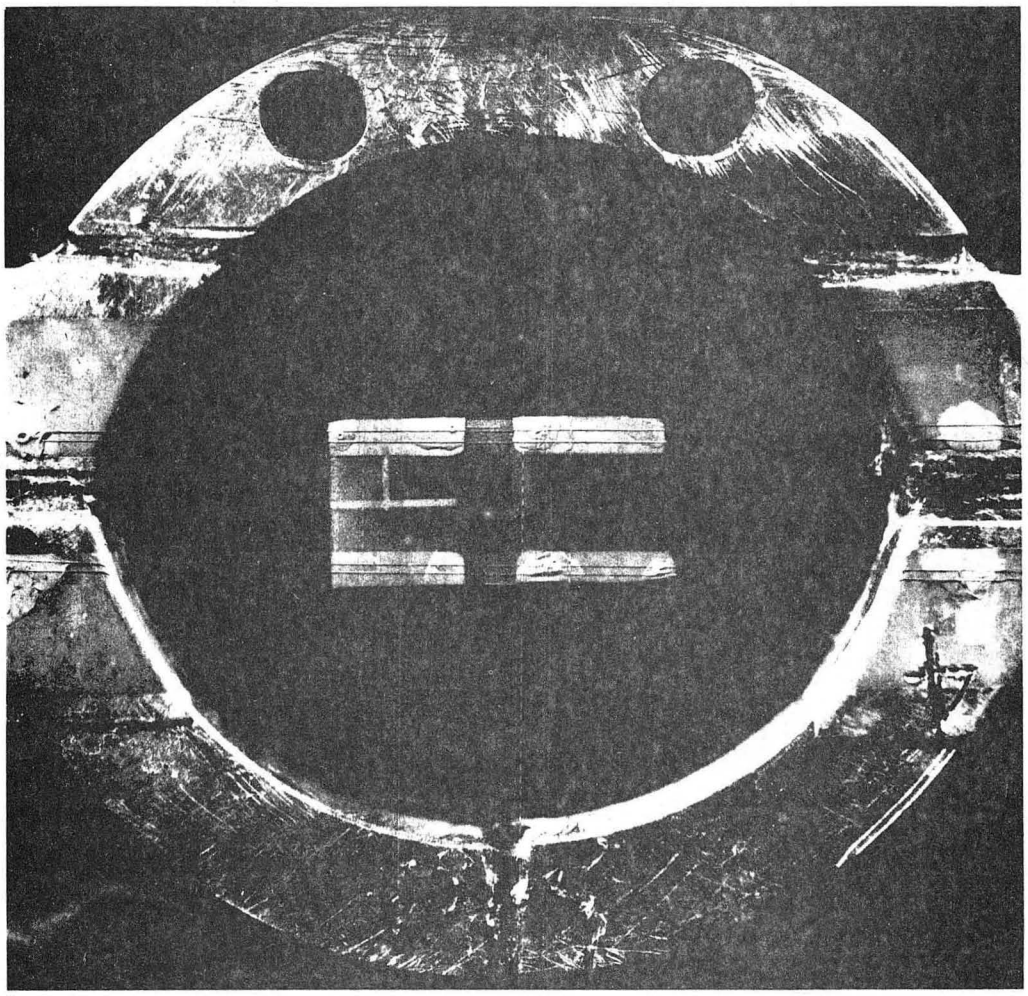

Fig. 11

LEGAL NOTICE

This report was prepared as an account of work sponsored by the United States Government. Neither the United States nor the United States Atomic Energy Commission, nor any of their employees, nor any of their contractors, subcontractors, or their employees, makes any warranty, express or implied, or assumes any legal liability or responsibility for the accuracy, completeness or usefulness of any information, apparatus, product or process disclosed, or represents that its use would not infringe privately owned rights.

TECHNICAL INFORMATION DIVISION
LAWRENCE BERKELEY LABORATORY
UNIVERSITY OF CALIFORNIA
BERKELEY, CALIFORNIA 94720